ELSEVIER

Journal of Organometallic Chemistry 557 (1998) 207–212

Journal of Organometallic Chemistry

Synthesis of novel ruthenium complexes of 2,2′-bis(diphenylphosphinomethyl)-1,1′-biphenyl and their catalytic hydrogenation reactions to α,β-unsaturated aldehydes

Rui-Xiang Li [a,]*, Kam-Chung Tin [a], Ning-Bew Wong [a], Thomas C.W. Mak [b], Ze-Ying Zhang [b], Xian-Jun Li [c]

[a] *Department of Biology and Chemistry, City University of Hong Kong, Tatchee Avenue, Kowloon, Hong Kong, China*
[b] *Department of Chemistry, Chinese University of Hong Kong, Satin, Hong Kong, China*
[c] *Department of Chemistry, Sichuan University, Chengdu 610064, China*

Received 23 July 1997; received in revised form 18 November 1997

Abstract

Three ruthenium complexes containing BISBI [2,2′-bis(diphenylphosphinomethyl)-biphenyl], $RuCl_2(PPh_3)(BISBI)$ **1**, $RuHCl(CO)(PPh_3)(BISBI)$ **2** and $RuH_2(CO)(PPh_3)(BISBI)$ **3**, had been prepared. Their compositions and structures were characterized by $^{31}P\{^1H\}$-NMR, ^1H-NMR and elemental analysis. Results of $^{31}P\{^1H\}$-NMR showed that the PPh_3 in complex **1** was completely dissociated and a dimer complex $[RuCl_2(BISBI)]_2$ was generated in $CDCl_3$ and C_6D_6 solutions. Molecular structure of **3** was also confirmed by single-crystal X-ray diffraction, the crystal belonged to a monoclinic system, $P2_1/n$ space group, $a = 16.771(3)$ Å, $b = 20.688(4)$ Å, $c = 17.139(3)$ Å, $\beta = 106.03(3)°$, $V = 5715(3)$ Å^3 and $Z = 4$. The hydrogenation results revealed that the three complexes showed much higher activities and selectivities than their analogous triphenylphosphine complexes for the hydrogenation of C=O bond in citral (3,7-dimethyl-2,6-octadienal) and cinnamaldehyde. © 1998 Elsevier Science S.A. All rights reserved.

Keywords: Ruthenium complex; 2,2′-bis(diphenylphosphinomethyl)-1,1-biphenyl; Hydrogenation; Citral; Cinnamaldehyde

1. Introduction

In recent decades, the synthesis and catalytic reaction of ruthenium complexes containing phosphines have been one of the most active research areas. A great number of papers have been published [1–4]. Ruthenium complexes containing one chelating bis(tertiary phosphine) ligand per metal atom are key species for catalytic homogeneous hydrogenation reactions, and spectacular success of such Ru(P–P) complexes in asymmetric hydrogenation of certain olefins, ketones and imines (where P–P is a chiral phosphine) have been demonstrated [5–11]. α,β-unsaturated aldehydes are known to be valuable intermediates in the field of fragrance and flavor chemistry, and very often involve the selective reduction of the carbonyl function in the multistep synthesis to new products [12]. Hydrogenation of the carbon–carbon double bond is readily achieved under mild conditions with high selectivity [13–15] whereas catalytic reduction of aldehyde group remains a challenging problem, and a few samples are reported for the formation of unsaturated alcohols [16–20]. The heterogeneous hydrogenation selectivity of C=O double bond in α,β-unsaturated aldehyde molecule over Ru/Al_2O_3 is very poor [21,22]. This paper presents three novel ruthenium complexes containing bidentate phosphine BISBI as well as the study the effect of coordination environment on catalytic activity and selectivity. The initial results show that ruthenium complexes containing BISBI have much higher activities and selectivities than the analogous ruthenium complexes of triphenylphosphine for the hydrognation of C=O bond in α,β-unsaturated aldehydes.

---

* Corresponding author. Fax: +852 27887406.

PII S0022-328X(97)00726-2

2. Experimental

2.1. Materials

All synthetic reactions were performed with standard Schlenk technique and under nitrogen atmosphere. Solvents were generally dried over appropriate drying agents and distilled under nitrogen prior to use. Reagent-grade PPh_3 was purchased from Aldrich, citral (97%) and cinnamaldehyde (98%) from Riedel–deHaën and were distilled before used. $RuCl_3 \cdot xH_2O$ (more than 42% Ru) was purchased from Kunming, China. Starting materials $RuCl_2(PPh_3)_3$ [23], $RuHCl(CO)(PPh_3)_3$ [24], $RuH_2(CO)(PPh_3)_3$ [24] and BISBI [25] were prepared according to the reported methods.

2.2. Analytical methods

The ^1H- and $^{31}P\{^1H\}$-NMR spectra were recorded on Bruker DPX 400 spectrometer at room temperature, 400.13 MHz for ^1H and 160.97 MHz for ^{31}P. The chemical shifts of ^{31}P-NMR were relative to 85% H_3PO_4 as external standard, ^1H relative to TMS as internal standard, with downfield shifts as positive. Elemental analyses were done on LECO CHN 900 element analyser. IR was recorded on Perkin Elmer 1600 spectrometer with KBr plate.

2.3. Catalytic hydrogenation

Appropriate amount of catalyst and substrate solutions were introduced into a stainless steel autoclave (100 ml) equipped with stirrer (Parr 4561 minireactor). The autoclave was evacuated and flushed with high purity hydrogen consecutively five times, then filled with hydrogen to the desired pressure. After the reaction solution was heated to the desired temperature, the stirrer was started (400 rpm) and reaction time was accounted. The reaction was quenched by immersing the reactor in an ice bath at the end of hydrogenation. The products were analyzed on GC (HP 5890 SERIES II) with an FID and a capillary column (HP-FFAP, 25 m × 0.2 mm × 0.33 µm), and the GC graphs were obtained with an HP 3396 INTEGRATOR. The components were identified by authentic sample on GC and GC–MS (HP 5890 GC with Series Mass Selective Detector).

3. Preparation of complexes

3.1. $RuCl_2(PPh_3)(BISBI)$ **1**

$RuCl_2(PPh_3)_3$ 0.96 g (1.0 mmol) and BISBI 0.54 g (1.0 mmol) were suspended in acetone (15 ml) and were refluxed for 1 h. The color of solid substance changed quickly from black to green during this time. At the end of reaction, the product was filtered, washed with acetone and diethyl ether, and recrystallized in toluene and n-hexane to give 0.73 g (74%) yield of **1** as green powder. Anal: calcd. for $C_{56}H_{47}Cl_2P_3Ru$: C, 68.30%; H, 4.82%. Found: C, 68.42%, H, 4.91%. $^{31}P\{^1H\}$NMR: δ (ppm) 54.8 (d), 52.9 (d), −6.7 (s), $J_{P-P} = 44$ Hz.

3.2. $RuHCl(CO)(PPh_3)(BISBI)$ **2**

$RuHCl(CO)(PPh_3)_3$ 0.19 g (0.2 mmol) and BISBI 0.11 g (0.2 mmol) were dissolved in 10 ml toluene. The solution was refluxed for 3 h, and the solution slowly changed from colorless to pale yellow during refluxing time. After the reaction completion, 30 ml n-hexane was added to the solution with syringe and no precipitate was observed. Then the solution was kept in a refrigerator overnight to form microcrystalline white needles. The crystals were filtered, washed with n-hexane and dried under vacuum to give 0.083 g (42%) of **2** as white needles. Anal.: Calc. for $C_{57}H_{48}ClOP_3Ru$: C, 69.96%; H, 4.95%; Found: C, 69.83%; H, 4.90%. $^{31}P\{^1H\}$-NMR: δ (ppm) 48.5 (dd), 32.9 (dd), and 26.8

Table 1
Experimental data for the X-ray diffraction studies

Formula	$C_{57}H_{49}OP_3Ru$
Formula weight	943.9
Space group	$P2_1/n$
a (Å)	16.771(3)
b (Å)	20.688(4)
c (Å)	17.139(3)
β (°)	106.03(3)
V (Å^3)	5715(2)
Z	4
D_{calc} (g cm^{-3})	1.097
Crystal size (mm)	0.22 × 0.22 × 0.25
Radiation	Mo $K\alpha$
Absorption coefficient	0.391 mm^{-1}
Transmition factor	0.741–1.000
$F(000)$	1952
Temperature (K)	293(2)
θ range for data collection	1.58–26.74°
Limiting indices	$0 \leq h \leq 21$, $-26 \leq k \leq 26$, $-21 \leq l \leq 20$
Reflections collected	16 687
Independent reflections	10 601 ($R_{int} = 0.1050$)
Observed reflection ($F > 6.0\sigma(F)$)	3595
Transmission factor	0.613/1.553
Quantity minimized	$\Sigma w(F_o - F_c)^2$
Refinement method	Full-matrix least-squares on F^2
Data/restraints/parameters	6928/0/560
Final R indices [$I > 2\sigma(I)$]	$R1 = 0.0690$, $wR2 = 0.1664$
R indices (all data)	$R1 = 0.1565$, $wR2 = 0.2224$
Goodness of fit on F^2	0.900
Extinction coefficient	0.0034(2)
Largest difference peak and hole	0.622 and −0.628 eÅ^{-3}

Table 2
Selected bond lengths and angles for $RuH_2(CO)(PPh_3)(BISBI)$

Bond	Lengths (Å) or angles(°)
Ru–C(1)	1.88 (1)
Ru–P(1)	2.33 (1)
Ru–P(2)	2.30 (1)
Ru–P(3)	2.38 (1)
C(1)–O	1.15 (1)
C(1)–Ru–P(1)	106.6(1)
C(1)–Ru–P(2)	96.0(1)
P(1)–Ru–P(2)	144.5(1)
C(1)–Ru–P(3)	91.7(1)
P(1)–Ru–P(3)	101.1(1)
P(2)–Ru–P(3)	105.4(1)

(t), $J_{P-Pcis} = 18$ Hz, $J_{P-Ptrans} = 296$ Hz; 48.4 (dd), 32.8 (dd), and 27.2 (t), $J_{P-Pcis} = 13$ Hz, $J_{P-Ptrans} = 296$ Hz; ^{1}H-NMR: δ (ppm) -6.95 (dt), $J_{H-Pcis} = 31$ Hz, and $J_{H-Ptrans} = 108$ Hz. IR: $\nu_{CO} = 1930$ cm^{-1} (vs), $\nu_{Ru-H} = 2038$ cm^{-1} (w).

3.3. *$RuH_2(CO)(PPh_3)(BISBI)$* **3**

It was synthesized by the same method as in complex **2**, but $RuH_2(CO)(PPh_3)_3$ 0.18 g (0.2 mmol) and BISBI 0.11 g (0.2 mmol) were used as the starting materials. Pale yellow microcrystals were obtained with 0.12 g (65%) yield. Anal.: Calc. for $C_{57}H_{49}OP_3Ru$: C, 72.52%, H, 5.23%; Found: C, 72.08%, H, 5.10%. $^{31}P\{^1H\}$NMR: δ (ppm) 58.9 (dd), 56.1 (dd) and 55.3 (t), $J_{P-Pcis} = 14$ Hz, $J_{P-Ptrans} = 232$ Hz; ^{1}H-NMR: δ (ppm) -7.9 (m, 1 H), $J_{Ha-Pcis} = 17$ and 18 Hz, $J_{Ha-Hb} = 8.1$ Hz; -9.5 (ds, 1 H), $J_{Hb-Pcis} = 33$ Hz, $J_{Hb-Ptrans} = 71$ Hz. IR, $\nu_{CO} = 1939$ cm^{-1} (vs).

3.4. *X-ray crystallographic analysis of* **3**

The crystal used for X-ray diffraction were grown from a 2:1 mixture solvent of toluene and *n*-hexane. The colorless plate crystal (0.22 × 0.22 × 0.25 mm) was covered with a thin layer of paraffin oil as a precaution against decomposition in air, and was mounted on a Rigaku RAXIS IIC imaging-plate diffractometer. Intensity data were collected at 293 K using graphite-monochromatized Mo $K\alpha$ ($\lambda = 0.71073$ Å) radiation from a rotating-anode generator operating at 50 kV and 90 mA. The θ range for data collection was 1.58–26.74°, 45° oscillation frames was in the range 0–135°, and the exposure was 10 min. per frame. A self-consistent semi-empirical absorption correction was applied by using the ABSCOR program. All calculation were performed with Siemens SHELXTL PLUS (PC Version) system. Structure refinement was based on F^2 for all 10601 reflections. A final *R*-factor is 0.0690, *wR* 0.1664, the largest and mean Δ/σ, and the largest difference peaks were presented in Tables 1 and 2 gave selected bond distances and angles.

4. Results and discussion

4.1. *Complex* **1**

The green solid complex was quite stable in air, but it was very unstable in solution when exposed in air, and the color of solution quickly changed from yellow-brown to brown and unidentified black precipitate was formed. When the complex was dissolved in organic solvents, such as, benzene and $CHCl_3$ under nitrogen, the color of solutions were brown, not green. The carbon and hydrogen analysis of the green product was consistent with the formula $RuCl_2(PPh_3)(BISBI)$. $^{31}P\{^1H\}$-NMR spectra in $CDCl_3$ or C_6D_6 exhibited two doublets at 54.8 and 52.9 ppm with coupling constant $J_{PP} = 44$ Hz and a strong singlet at -6.7 ppm. The former was a typical AB splitting pattern of dimer ruthenium-phosphine complexes with chloride bridges [5,26], and the latter was assigned to free PPh_3. The integration ratio of two doublets to singlet was roughly 2. Moreover, except for the two doublets and the singlet of free PPh_3 in this solution, any peaks of **1** could not be observed on the spectra.

However, besides of the two doublets of dimer and the singlet of free PPh_3, the ^{31}P-NMR spectra appeared two very weak wide doublets at 13.2 and 47.2 ppm and a wide singlet at 71.2 ppm at -20.0°C. When the temperature was further decreased to -55°C, the intensities of the three new wide peaks were greatly increased and sharpened, the $^{31}P\{^1H\}$-NMR spectra clearly exhibited two doublets of doublet at 13.2 and 47.2 ppm and a unsymmetric quartet at 71.2 ppm. Their coupling constants were $J_{Px-Pa} = 20$ Hz and $J_{Pb-Pa} = 306$ Hz at 13.2 ppm, $J_{Px-Pb} = 38$ Hz and $J_{Pa-Pb} = 308$ Hz at 47.2 ppm, and $J_{Pa-Px} = 20$ Hz and $J_{Pb-Px} = 38$ Hz at 71.2 ppm. This result confirmed that complex **1** was only stable in solution at very low temperature. However, the peak intensity of the AB splitting pattern of dimer was still greater than the new ABX splitting pattern (the ratio was about 2:1) at -55°C. Furthermore, when the equil molar ratio PPh_3 was dissolved in the $CDCl_3$ solution of **1**, the color of solution changed from brown to green-yellow, the singlet peak of PPh_3 was enhanced, two doublets at 54.8 and 52.9 ppm were not remarkable change, but three very weak wide peaks with ABX splitting pattern were appeared at 13.0, 47.2 and 71.2 ppm. Attempts to isolate the dimer complex from its oganic solution by adding diethyl ether or *n*-hexane were unsuccessful, only the original green solid complex **1** was recovered. These results suggested that PPh_3 in the complex was almost completely dissociated in organic solvent and

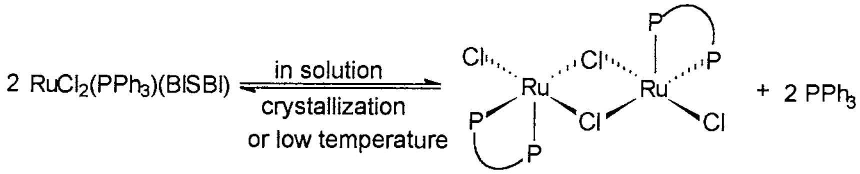

Fig. 1. Conversion of $RuCl_2(PPh_3)(BISBI)$ to $[RuCl_2(BISBI)]_2$ in solution.

the unstable intermediate was subsequently dimerized at room temperature, and the low temperature and crystallization was favourable to the association of PPh_3 and dimer to form mononuclear complex **1** again. The proposed conversion to dimer structure could be seen in Fig. 1. This phenomenon has also been reported in many phosphine complexes of ruthenium [26–28], but the degree of dissociation of PPh_3 was usually much smaller at room temperature. According to our knowledge, the complete dissociation of PPh_3 in solution has not yet been reported. The large chelating angle of the ligand [29] and the big chelating ring (9-membered ring) of **1** may be responsible for the unstable molecular structure in solution.

4.2. Complex 2

The complex **2** was stable in solution as well as in solid state. However, the yellow solution would gradually changed to dark brown color after it was exposed in air for two days. ^{1}H-NMR of this complex in C_6D_6 showed a doublet of triplets at -6.95 ppm and coupling constants were $J_{H-Pcis} = 31$ Hz and $J_{H-Ptrans} = 108$ Hz. The results indicated that one phosphorus atom was in the *trans*-position to the hydride and two phosphorus atoms were in the *cis*-position. This also reflected that the two phosphorus atoms in the *cis*-position to this hydride would be the two phosphorus atoms of BISBI according to the symmetry of peaks. However, $^{31}P\{^1H\}$-NMR showed two sets of peaks with the same intensity and the same splitting pattern. The results suggested that the two sets of peaks should be assigned to two isomers with the same phosphorus configuration in the steric structure. ^{1}H- and $^{31}P\{^1H\}$-NMR had exhibited that the hydrogen atom and the three phosphorus atoms were on the same plane and were arranged in meridian form with two phosphorus atoms of BISBI. The position exchange of CO and Cl in the molecule could not vary the chemical environment of the three phosphorus atoms. The two isomers should result from the two distorted phenyl rings in the chelating ring back-bone of BISBI. The steric structure of **2** can be proposed in Fig. 2. Compared to the IR spectra of $RuHCl(CO)(PPh_3)_3$ ($\nu_{CO} = 1923$ and $\nu_{Ru-H} = 2014$ cm^{-1}), that the absorption peak of CO in **2** was shifted to higher wave number which indicated that the back-donor electron from Ru was decreased in CO π anti-bond orbit after triphenylphosphine was substituted with BISBI. The IR absorption peak of Ru–H bond was also shifted to high wave number.

4.3. Complex 3

^{1}H-NMR of this complex showed multiplets at -7.9 ppm with the coupling constants $J_{Ha-Pcis} = 17$ and 18 Hz and $J_{Ha-Hbcis} = 8$ Hz, and a doublet of sextet at -9.5 ppm with coupling constants $J_{Hb-Pcis} = 33$ Hz and $J_{Hb-Ptrans} = 70$ Hz, $J_{Ha-Hbcis} = 8$ Hz. The integration ratio of H_a to H_b signals was 1:1. According to the ^{1}H-NMR spectra and the coupling constants, it could be reasonably suggested that the two coordinated hydrogen atoms were in *cis*-position to each other, H_a was in *cis*-position to three phosphorus atoms, H_b was in *trans*-position to one phosphorus atom and in *cis*-position to two other phosphorus atoms.

$^{31}P\{^1H\}$-NMR spectra showed two doublets of doublets at 58.8 and 56.1 ppm and a triplet at 48.7 ppm with the coupling constants $J_{P-Pcis} = 14$ Hz and $J_{P-Ptrans} = 232$ Hz. The result also indicated that two phosphorus atoms were in *trans*-position to each other and one in *cis*-position to another two phosphorus atoms. According to the $^{31}P\{^1H\}$-NMR and ^{1}H-NMR results, the molecule structure of **3** was proposed in Fig. 3. The IR of **3** showed that the absorption peak of carbonyl shifted to lower wave number ($\nu_{CO} = 1939$ cm^{-1}) in relative to $RuH_2(CO)(PPh_3)_3$ ($\nu_{CO} = 1942$

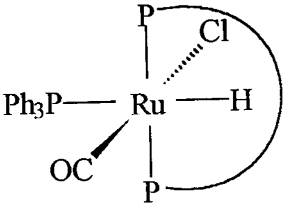

Fig. 2. Proposed structure of **2**.

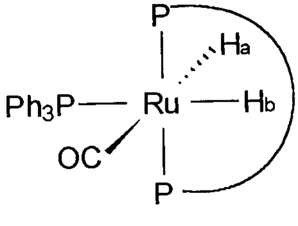

Fig. 3. Proposed structure of **3**.

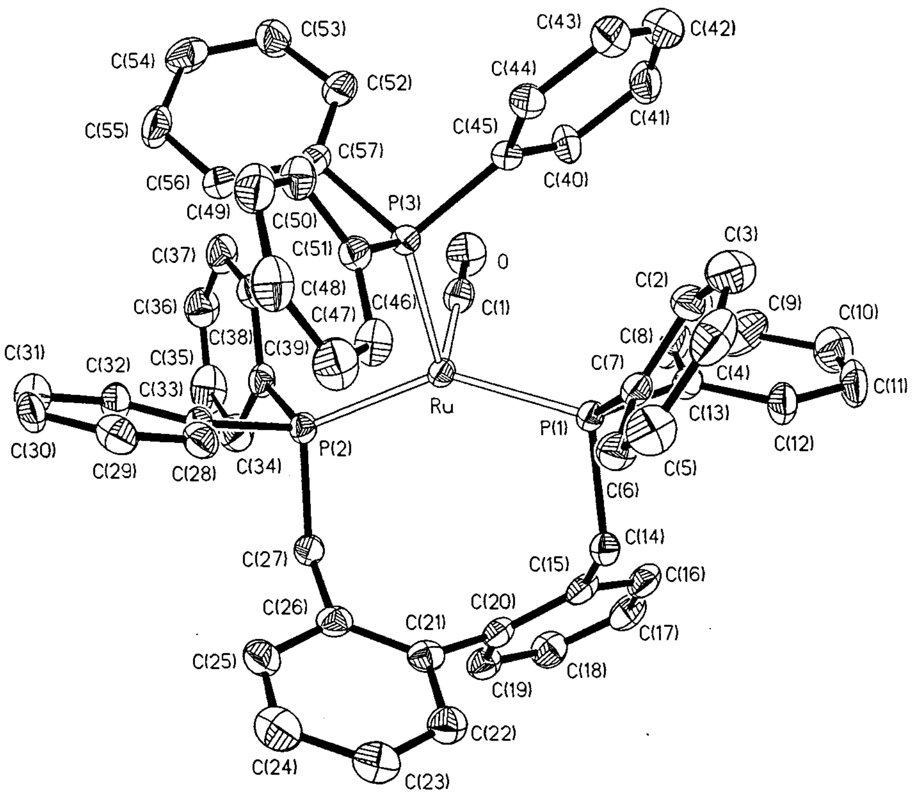

Fig. 4. An ORTEP drawing of the complex **3**.

cm^{-1}). However, the absorption of carbonyl group was too strong, so that the Ru–H absorption was overlapped with the carbonyl peak and could be not observed in IR spectra.

The results of single-crystal X-ray diffraction were listed in Tables 1 and 2 and Fig. 4. It was consistent with the structural analysis by NMR spectra. The two phosphorus atoms of BISBI were in *trans* position. If two hydrogen atoms were added in the structure, the configuration of the complex was a distorted octahedron. The bond angle between two P–Ru bonds coordinated by BISBI was 144.6°, which was much less than 180° because of the distort tension of chelating ring and pressure raised by the large volume of the triphenylphosphine group.

4.4. Hydrogenation of citral and cinnamaldehyde catalyzed by Ru complexes *1*, *2* and *3*

Hydrogenation results were shown in Table 3. The substitution of PPh_3 by BISBI had improved both the catalytic activities and selectivities of ruthenium complexes **1**, **2** and **3** for the hydrogenation of C=O bond in α,β-unsaturated aldehydes to form allylic alcohols. The catalytic activities of **1** and **2** were much higher than the analogous triphenylphosphine complexes. It was reasonable to suggest that the large chelating angle and chelating ring (nine-membered chelating ring) enhanced the dissociation of PPh_3 in solution which had been verified by $^{31}P\{^1H\}$-NMR for **1**. The generated dimer could be easily transfered into active catalytic species when it further reacted with hydrogen under ambient conditions. Besides of the large chelating contributing to improve the catalytic activities and selectivities, the electronic factor seemed to play a important role. When the coordination environment of ruthenium was further modified with carbonyl and hydride, such as **2** and **3**, **2** showed higher catalytic activity than **1**. However, the catalytic activity of **3** was sharply decreased. The carbonyl absorption of **3** in IR spectra was shifted to higher wave number had indicated that back-donored electron from ruthenium decreased when the chloride in **2** was substituted by the hydride. This means that the electronic density of ruthenium in **3** was lower than in **2**. It might be reasonable to suggest that the lower electronic density of ruthenium in **3** was not favourable to the catalytic reaction.

Acknowledgements

This work was supported by City University of Hong Kong, Chinese University of Hong Kong and Sichuan University, China.

Table 3
Hydrogenation of α,β-unsaturated aldehydes

Catalysts	Citral[a]		Cinnamaldehyde[b]	
	Conversion (%)	Selectivity[c] (%)	Conversion (%)	Selectivity[c] (%)
$RuCl_2(PPh_3)_3$	28	23	25	73
$RuCl_2(PPh_3)$(BISBI)	41	80	48	86
$RuHCl(CO)(PPh_3)_3$	4.1	8.8	9.9	76
$RuHCl(CO)(PPh_3)$(BISBI)	62	60	85	73
$RuH_2(CO)(PPh_3)_3$	0.0	—	4.2	62
$RuH_2(CO)(PPh_3)$(BISBI)	3.3	40	11	88

Reaction conditions: substrate 2.0 ml, temp.: 50°C.

[a] Benzene: 8.0 ml, time: 2 h, H_2 pressure: 20 kg cm^{-2}, catalyst conc. 2.0×10^{-3} M.

[b] Cyclohexane: 8.0 ml, time: 1 h, H_2 pressure: 30 kg cm^{-2}, catalyst conc. 1.0×10^{-3} M.

[c] Selectivity in allylic alcohol.

References

[1] T.A. Stephenson, G. Wilkinson, J. Inorg. Nuclear Chem. 28 (1966) 1945.
[2] P.S. Hallman, B.R. McGarvey, G. Wilkinson, J. Chem. Soc. (1968) 3143.
[3] H.A. Mayer, W.C. Kaska, Chem. Rev. 94 (1994) 1239.
[4] B.R. James, A. Pacheco, S.J. Rettig, J. Mol. Catal. 41 (1987) 147.
[5] A.M. Joshi, I.S. Thorburn, S.J. Rettig, B.R. James, Inorg. Chim. Acta 198–200 (1992) 283.
[6] R. Noyori, H. Takaya, Acc. Chem. Res. 23 (1990) 345.
[7] A.M. Joshi, K.S. MacFarlane, B.R. James, J. Organomet. Chem. 488 (1995) 161.
[8] B.R. James, D.K.W. Wang, Can. J. Chem. 58 (1980) 245.
[9] T. Ohta, H. Takaya, R. Noyori, Tetrahedron lett. 31 (1990) 7189.
[10] K. Na, S. Huh, K. Sung, M. Jun, Polyhedron 15 (1996) 1841.
[11] M.T. Ashby, J. Halpern, J. Am. Chem. Soc. 113 (1991) 589.
[12] K. Bauer, D. Garbe, Ullman Encyclopedia, 3rd edn. vol. A11, VCH: New York, 1988, p. 141.
[13] B.R. James, Homogenous Hydrogenation, Wiley, New York, 1973.
[14] D.M. Bretensky, J.M. Stryker, Tetrahedron Lett. 30 (1989) 5677.
[15] Z. Brouckova, M. Czakova, M. Capka, J. Mol. Catal. 30 (1989) 241.
[16] T. Mizoroki, K. Seki, S. Meguro, A. Ozaki, Bull. Chem. Soc. Jpn. 50 (1977) 2148.
[17] B.R. James, R. Morris, J. Chem. Soc. Chem. Commun. (1978) 929.
[18] K. Hotta, J. Mol. Catal. 29 (1985) 105.
[19] E. Farnetti, J. Kaspar, R. Spogliarich, M. Graziani, M. Pesce, J. Mol. Catal. 43 (1987) 35.
[20] T. Suarez, B. Fontal, J. Mol. Catal. 45 (1988) 345.
[21] L. Mercadante, G. Neri, C. Milone, A. Donato, S. Galvagno, J. Mol. Catal. A Chem. 105 (1996) 93.
[22] G. Neri, L. Mercadante, C. Milone, R. Pietropaolo, S. Galvagno, J. Mol. Catal. A Chem. 108 (1996) 41.
[23] P.S. Hallman, T.A. Stephenson, G. Wilkinson, Inorg. Synth. 12 (1970) 237.
[24] J.J. Levison, S.D. Robinson, J. Chem. Soc. (A), (1970) 2947.
[25] T.A. Puckertte, T.J. Devon, G.W. Phillips, J.L. Stavinoha, U.S. Patent, 4879416 (1989), Chem. Abstr. 112 (1989) 217269k.
[26] A. Mezzetti, G. Consiglio, J. Chem. Soc. Chem. Commun. (1991) 1675.
[27] P.W. Armit, A.S.F. Boyd, T.A. Stephenson, J. Chem. Soc. Dalton (1975) 1661.
[28] C.W. Jung, P.E. Garrou, P.R. Hoffman, K.G. Caulton, Inorg. Chem. 23 (1984) 726.
[29] C.P. Casey, G.T. Whiteker, M.G. Melville, L.M. Petrovich, J.A. Gavney Jr., D.R. Powell, J. Am. Chem. Soc. 114 (1992) 5535.